# DEEP SPECTRUM CARTOGRAPHY USING QUANTIZED MEASUREMENTS

Subash Timilsina, Sagar Shrestha, and Xiao Fu

School of EECS, Oregon State University Corvallis, OR 97331, USA

(timilsis, shressaq, xiao.fu)@oregonstate.edu

#### ABSTRACT

Spectrum cartography (SC) techniques craft multi-domain (e.g., space and frequency) radio maps from limited measurements, which is an ill-posed inverse problem. Recent works used low-dimensional priors such as a low tensor rank structure and a deep generative model to assist radio map estimation—with provable guarantees. However, a premise of these approaches is that the sensors are able to send real-valued feedback to a fusion center for SC-yet practical communication systems often use (heavy) quantization for signaling. This work puts forth a limited feedback-based SC framework. Similar to a prior work, a generative adversarial network (GAN)based deep prior is used in our framework for fending against heavy shadowing. However, instead of using real-valued feedback, a random quantization strategy is adopted and a maximum likelihood estimation (MLE) criterion is proposed. Analysis shows that the MLE provably recovers the radio map, under reasonable conditions. Simulations are conducted to showcase the effectiveness of the proposed approach.

*Index Terms*— Radio maps, spectrum cartography, deep neural network, generative adversarial network, quantized data.

### 1. INTRODUCTION

Spectrum cartography (SC) aims to craft a multi-domain (e.g., frequency, time, and space) radio interference propagation map from limited and sparsely deployed sensors [1,2]. SC is considered central for establishing radio frequency (RF) awareness in complex communication scenarios, as the radio maps can assist effective wireless resource allocation/management in crowded and interference limited environments [3].

From a signal processing perspective, SC is an inverse problem—recovering the high-dimensional multi-domain radio map (which is a high-order tensor) from limited samples is clearly ill-posed. In the past decade, many solutions were proposed to solve the recovery problem; see, e.g., [1, 4–9]. In essence, these methods used prior information of the radio map to come up with its parsimonious and succinct representations (by using, e.g., dictionary learning [7], kernel modeling [10], and low-rank tensor modeling [1]). Recently, the work in [2] used deeply learned priors of the radio maps under heavily shadowed scenarios, where handcrafted priors often struggle to accurately represent such complex data. Notably, the work in [1,2] also established recoverability guarantees of their methods, which sheds lights on key tradeoffs in radio map engineering.

The recent developments of SC, especially the integration with deep priors to fight shadowing, have been encouraging. Nonetheless, the vast majority of the existing SC methods work under the

This work is supported in part by the National Science Foundation (NSF) under Project NSF CCF-2210004.

premise that the sensors are able to send real-valued power spectrum measurements to a fusion center. In practice, this type of real-valued full-precision measurements are rarely used, as they induce heavy communication overheads. In practice, such measurements are often quantized before being fed back to the fusion center [3,11]. In the past decade, a number of attempts were made towards using quantized feedback for RF awareness tasks; see, e.g., [10,12,13]. In particular, the work in [10] used a kernel regression method to deal with quantized measurements-based SC. However, the method in [10] assumed that the power spectral signature of every emitter is known, but estimating such signatures is a highly nontrivial task [6,14]. How to recover radio maps under a fully blind setting (i.e., without knowing the emitters' spectral signatures *a priori*) using quantized measurements with provable guarantees remains an open challenge.

In this work, we propose a new SC approach that generalizes the recent deep SC method in [2] in a nontrivial way. To be specific, we use the deep prior-based low-dimensional representation of SC from [2], as it is proven robust to heavy shadowing. However, unlike the work in [2] that uses real-valued feedback, we assume that the sensors quantize the sensed power spectral density in each frequency using only a few bits. We adopt a random quantization strategy that is commonly used in quantized compressive sensing [15-19] and formulate the recovery problem using the maximum-likelihood estimation (MLE) principle. To tackle the proposed MLE criterion, we design a simple and easy-to-implement alternating optimization algorithm. More importantly, we show that the formulated criterion ensures recovering the ground-truth radio map (up to bounded errors) under challenging scenarios, e.g., when the deep prior does not exactly match the ground truth. Simulations using realistic physical models corroborate our design goals and theoretical claims.

### 2. PROBLEM STATEMENT AND BACKGROUND

We consider the problem of recovering a spatio-spectral radio map from N sensors that are sparsely deployed over the space; see similar problem settings in [1,2,4-9]. For simplicity, we consider the case where the spatial domain is a 2D rectangle and is discretized into  $I \times J$  grids. Every grid admits a power spectral density (PSD) that is measured over K frequency bins. Hence, the radio map that we hope to estimate is a third-order tensor  $\underline{X} \in \mathbb{R}^{I \times J \times K}$ , where  $\underline{X}(i,j,k)$  is the PSD of the signal received at position (i,j) and the kth frequency bin. That is, every fiber [20] of the tensor,  $\underline{X}(i,j,:)$ , represents the PSD of the received signal measured at the location (i,j). We also denote  $\Omega = \{(i,j)|i \in [I], j \in [J]\}$  as the set of locations where the sensors are placed. Note that

$$|\Omega| = N \ll IJ$$

normally holds, as the number of sensors is often small. Assume that every sensor acquires the full PSD  $\underline{X}(i_s, j_s, :)$  at its location

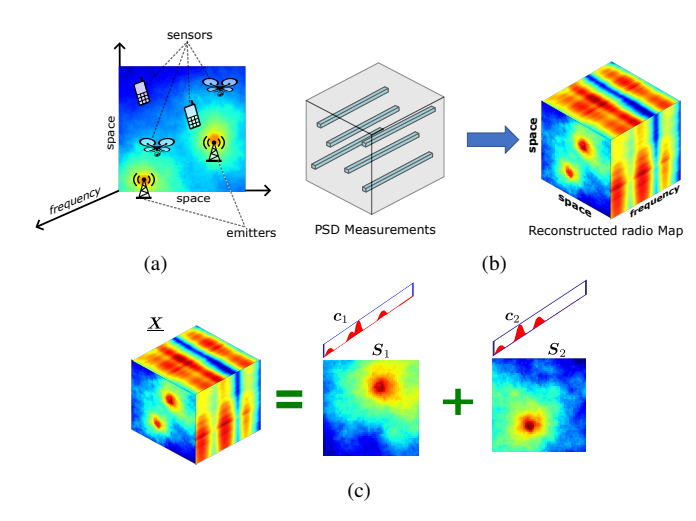


**Fig. 1**: (a) An SC scenario with 2 emitters and 4 sensors. (b) Left: Measurements acquired by sensors. Right: the radio map to recover (adapted from [2]). (c) Illustration of (1) (adapted from [1,2]).

 $(i_s,j_s)$  for  $s=1,\ldots,N$ . If the sensors are able to transmit real-valued feedback to the fusion center, the goal of SC is to recover the full  $\underline{\boldsymbol{X}}$  from the tensor fibers  $\{\underline{\boldsymbol{X}}(i,j,:)\}_{(i,j)\in\Omega}$  at the fusion center.

The scenario and problem statement are illustrated in Fig.1 (a)-(b). We should mention that although we considered a 2D spatial domain, the idea can be generalized to cover 3D spatial domains in a straightforward manner.

#### 2.1. Provable SC using Full-Precision Measurements

The work in [1,2] proposed two recoverability-guaranteed SC approaches. Both of their methods started with a physical model of the radio map that has been widely used in the literature [1,2,10,21]. The radio map model (in the noiseless case) is as follows:

$$\underline{\underline{X}}(i,j,k) = \sum_{r=1}^{R} S_r(i,j) c_r(k) \iff \underline{\underline{X}} = \sum_{r=1}^{R} S_r \circ c_r, \quad (1)$$

where "o" denotes the outer product (i.e.,  $[\boldsymbol{U} \circ \boldsymbol{v}]_{i,j,k} = \boldsymbol{U}(i,j)\boldsymbol{v}(k)$  for a matrix  $\boldsymbol{U}$  and a vector  $\boldsymbol{v}$ ),  $\boldsymbol{S}_r \in \mathbb{R}^{I \times J}$  is the spatial loss field (SLF) of the rth emitter,  $\boldsymbol{c}_r \in \mathbb{R}^K$  is the PSD of emitter r, and R is the number of emitters. The SLF captures the spatial power propagation characteristics of an emitter, and the PSD reflects the emitter's spectral band occupancy. Fig. 1 (c) illustrates the model in (1). The model means that the spatial and spectral information of the radio map can be decomposed into their own latent factors. This is reasonable when the frequency band is not very wide, where the power propagation is still coherent across the neighboring frequency bins [6,14].

Many works under the model in (1) were proposed in the past decade; see, e.g., [1, 4–7]. Most of the early works did not have recoverability guarantees of  $\underline{X}$  using observations over  $\Omega$ . More recently, the work in [1] used a block-term tensor recovery perspective and formulated the problem as follows:

$$\min_{\{\boldsymbol{c}_r, \boldsymbol{A}_r, \boldsymbol{B}_r\}_{r=1}^R} \left\| \underline{\boldsymbol{M}}_{\text{sens}} \circledast \left( \underline{\boldsymbol{X}} - \sum_{r=1}^R (\boldsymbol{A}_r \boldsymbol{B}_r^\top) \circ \boldsymbol{c}_r \right) \right\|_{\Gamma}^2, \quad (2)$$

where  $\underline{\boldsymbol{M}}_{\mathrm{sens}}$  is a mask tensor such that  $\underline{\boldsymbol{M}}_{\mathrm{sens}}(i,j,:) = \boldsymbol{1} \in \mathbb{R}^K$  if  $(i,j) \in \boldsymbol{\Omega}$  and  $\underline{\boldsymbol{M}}_{\mathrm{sens}}(i,j,:) = \boldsymbol{0}$  otherwise, and  $\boldsymbol{\otimes}$  denotes the

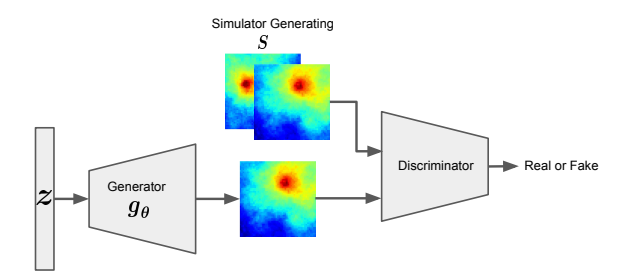


**Fig. 2**: Learning  $S_r = g_{\theta}(z)$  using simulated SLFs and the generative adversarial network (GAN); see other approaches for learning such generative models in [2].

Hadamard product. The idea of (2) is to model the SLFs as low-rank matrices, i.e.,  $S_r = A_r B_r^{\top}$  with  $\mathrm{rank}(A_r) = \mathrm{rank}(B_r) = L \ll \min\{I,J\}$ . The work presented the first provable blind SC approach. The caveat is that the low-rank model for the SLFs may not always hold, especially when the shadowing effects are severe. To overcome this challenge, the work in [2] modeled the individual SLFs using a deep generative model and adapted the criterion in (2) to the following:

$$\min_{\{\boldsymbol{c}_r, \boldsymbol{z}_r\}_{r=1}^R} \left\| \underline{\boldsymbol{M}}_{\text{sens}} \circledast \left( \underline{\boldsymbol{X}} - \sum_{r=1}^R \boldsymbol{g}_{\boldsymbol{\theta}}(\boldsymbol{z}_r) \circ \boldsymbol{c}_r \right) \right\|_F^2, \quad (3)$$

where  $g_{\theta}(\cdot): \mathbb{R}^D \to \mathbb{R}^{I \times J}$  is a generative deep neural network that links every SLF with a D-dimensional embedding  $z_r \in \mathbb{R}^D$  with D << IJ. The model  $g_{\theta}(\cdot)$  is learned from simulated SLFs that cover a wide range of shadowing situations using neural learners, e.g., the generative adversarial network (GAN) [22] or the autoencoder [23]; see Fig. 2 for illustration and [2] for details. Such a data-driven prior is often more resilient to heavy shadowing in practice. Notably, recoverability of the radio map was also established with the deep model  $g_{\theta}$  in [2].

### 2.2. SC Methods using Quantized Data

Both the methods in [1] and [2] are based on the assumption that the sensors can feedback full-precision real-valued PSD measurements. However, this is unrealistic, as such real-valued feedback is costly in terms of communication overhead. The works in [10, 12, 13] considered using quantized feedback for RF awareness tasks. In particular, the work in [10] used kernel regression for reconstructing the radio map with heavily quantized data. However, this method assumes that the fusion center has the full knowledge of the PSDs of the emitters. Nonetheless, estimating such PSDs *per se* is a highly nontrivial problem; see [6, 14]. Furthermore, the existing methods using quantized measurements for RF awareness in general lack theoretical supports. To our best knowledge, the problem of provable blind SC (i.e., SC under the setting where the emitters' PSDs are unknown) using quantized feedback has not been addressed.

#### 3. PROPOSED APPROACH

In this section, we propose a nontrivial generalization of the formulation in (3) to handle quantized measurements.

#### 3.1. Gaussian Quantization

We propose to employ the random quantization scheme that is often used in quantized compressive sensing and matrix/tensor completion, e.g., [15–19]. In the following, we denote the ground-truth radio map by  $\underline{X}^{\natural}$ , which we wish to recover. Then, our quantization function  $\mathcal{G}(\cdot)$  is as follows:

$$\underline{\underline{Y}}(i,j,k) = \mathcal{G}(h(\underline{\underline{X}}^{\natural}(i,j,k)) + \underline{\underline{V}}(i,j,k))$$

$$\mathcal{G}(x) = q, \text{ if } b_{q-1} < x < b_q, \quad q \in [Q] = \{1, \dots, Q\},$$

$$(4)$$

where we propose to use  $h(x) = \log(x+a)$  for "squeezing" the dynamic range of the radio map, a is a pre-specified offset,  $\underline{V}(i,j,k) \sim \mathcal{N}(0,\sigma^2)$  for all i,j,k are i.i.d. noise terms, and  $\{b_q\}_{q=0}^Q$  are the pre-specified quantization bins. Adding noise before quantization is called *dithering* in signal processing [24]. Roughly speaking, dithering introduces more information to help recognize the values that are close to the quantization boundaries. This technique is also widely used in quantized matrix/tensor completion; see, e.g., [15–19].

Denote  $\underline{M}^{\natural} = h(\underline{X}^{\natural})$ , where  $h(\cdot)$  is applied component-wise onto  $X^{\natural}$ . Then, the entries of Y have the following distribution:

$$\underline{Y}(i,j,k) = q$$
, w.p.  $f_q(\underline{M}(i,j,k)), \forall (i,j) \in \Omega$  (5)

where  $f_q$  is defined using the cumulative distribution function (CDF) (i.e., the  $\Phi$ -function) of the standard Gaussian variable; i.e.,

$$f_{q}(\underline{\boldsymbol{M}}(i,j,k)) = \mathbb{P}(\underline{\boldsymbol{Y}}(i,j,k) = q \mid \underline{\boldsymbol{M}}(i,j,k))$$
  
=  $\Phi(b_{q} - \underline{\boldsymbol{M}}(i,j,k)) - \Phi(b_{q-1} - \underline{\boldsymbol{M}}(i,j,k)).$  (6)

Using the above quantization strategy, we formulate our radio map recovery problem as an MLE criterion:

$$\min_{\{\boldsymbol{z}_r, \boldsymbol{c}_r\}_{r=1}^R} F_{\boldsymbol{\Omega}, \underline{\boldsymbol{Y}}}(\boldsymbol{Z}, \boldsymbol{C}), \quad \text{subject to } \boldsymbol{C} \geq \boldsymbol{0}, \tag{7}$$

where  $Z = [z_1, \ldots, z_R], C = [c_1, \ldots, c_R]$  and  $F_{\Omega, \underline{Y}}(Z, C)$  is expressed as

$$-\sum_{(i,j)\in\boldsymbol{\Omega}}\sum_{k=1}^K\sum_{q=1}^Q\mathbb{1}_{\underline{\boldsymbol{Y}}(i,j,k)=q}\log(f_q\big(h([\sum_{r=1}^R\boldsymbol{g}_{\boldsymbol{\theta}}(\boldsymbol{z}_r)\circ\boldsymbol{c}_r]_{i,j,k})\big)).$$

The constraint on C is added per its physical meaning, as it consists of the PSDs of the emitters. Here, the deep generative model of the SLFs, i.e.,  $g_{\theta}(\cdot)$  is adopted for the same reason as in [2]—i.e., fending against heavy shadowing.

### 3.2. Algorithm Design

To handle the proposed MLE problem, we propose an alternating optimization algorithm. The update of C in the kth iteration can be carried out as follows:

$$\boldsymbol{C}^{(k+1)} \leftarrow \max(\boldsymbol{C}^{(k+1)} \leftarrow \boldsymbol{C}^{(k)} - \alpha^{(k)} \overline{\nabla}_{\boldsymbol{C}} F_{\boldsymbol{\Omega}, \underline{\boldsymbol{Y}}}(\boldsymbol{Z}^{(k)}, \boldsymbol{C}^{(k)}), \boldsymbol{0}),$$

where  $\overline{\nabla}_{C}(\cdot)$  is a gradient-related direction—which could be constructed following any off-the-shelf first-order optimization algorithm, e.g., Adagrad [25], Adadelta [26], Adam [27],  $\alpha^{(k)}$  is the step size, and  $\max(C^{(k+1)}, \mathbf{0})$  projects  $C^{(k+1)}$  onto the nonnegative orthrant. Similarly, the Z-update can be done as follows:

$$\boldsymbol{Z}^{(k+1)} \leftarrow \boldsymbol{Z}^{(k)} - \beta^{(k)} \overline{\nabla}_{\boldsymbol{Z}} F_{\boldsymbol{\Omega}, \underline{\boldsymbol{Y}}}(\boldsymbol{Z}^{(k)}, \boldsymbol{C}^{(k)}).$$

The algorithm is summarized in Algorithm 1.

#### 3.3. Performance Characterization

In this subsection, we provide recoverability characterization of the MLE estimator in (7). The following theorem states our main result:

**Theorem 1** Assume that  $g_{\theta}(\cdot)$  is P-Lipschitz continuous, and that  $\Omega \subseteq \{(i,j)|i \in [I], j \in [J]\}$  is uniformly sampled with replacement, where  $|\Omega| = N$ . Let  $\underline{Y}$  be the quantized radio map tensor obtained from (5). Denote the set of solutions as follows:

$$\mathcal{X}_{R,\boldsymbol{g_{\boldsymbol{\theta}}}} := \Big\{\underline{\boldsymbol{X}} = \sum_{r=1}^{R} \widetilde{\boldsymbol{S}}_r \circ \widetilde{\boldsymbol{c}}_r \; \bigg| \; \max_{i,j,k} |\underline{\boldsymbol{X}}(i,j,k)| \leq \alpha, \; \widetilde{\boldsymbol{S}}_r = g_{\boldsymbol{\theta}}(\boldsymbol{z}_r),$$

$$\|\boldsymbol{z}_r\|_2 \le \zeta, \|\boldsymbol{g}_{\boldsymbol{\theta}}(\boldsymbol{z}_r)\|_F \le \beta, \|\widetilde{\boldsymbol{c}}_r\|_2 \le \kappa, \forall r \in [R]$$
 (8)

Suppose that  $\min_{\underline{\widetilde{X}} \in \mathcal{X}_{R,g_{\theta}}} \| \underline{\widetilde{X}} - \underline{X}^{\natural} \|_F \leq \nu$ , where  $\nu \geq 0$  is a constant. With probability  $1 - \delta$ , the following holds:

$$\frac{\|\underline{\boldsymbol{X}}^* - \underline{\boldsymbol{X}}^{\natural}\|_F^2}{IJK} \le \frac{C_1\sqrt{R}\tau + C_2\sqrt{8\log(\frac{1}{\delta})}}{K\sqrt{N}} + C_3\nu,$$

where  $\underline{X}^* = \sum_{r=1}^R g_{\theta}(z_r^*) \circ c_r^*, \{z_r^*, c_r^*\}_{r=1}^R$  is an optimal solution of the MLE over  $\mathcal{X}_{R,g_{\theta}}$ ;  $C_1$  and  $C_3$  are constants that depend upon the parameters a,  $\sigma^2$ , and  $\alpha$ ;  $C_2$  depends on  $\sigma^2$  and  $\alpha$ ; and

$$\tau = 1 + 3\sqrt{(K+D)\log(3\sqrt{R}(\beta+\kappa)) + K\log(\kappa) + D\log(P\zeta)}.$$

*Proof Sketch:* Our proof generalizes the classic quantized matrix completion's recoverability analysis (see, e.g., [19]) to incorporate deep generative models and the case using radio map fiber sampling. The sketch of our proof can be summarized in the following three steps: First, the mean squared error (MSE) between the recovered tensor  $\underline{X}^*$  and ground-truth tensor  $\underline{X}^{\natural}$  is bounded by estimating the Kullback-Leibler (KL)-divergence between the two distributions  $f_q(h(\underline{X}^*))$  and  $f_q(h(\underline{X}^{\natural}))$ . Second, the KL-divergence is upper bounded by the sum of estimation error, generalization error and approximation error terms. Third, the generalization error is upper bounded by using the Rademacher complexity of the deep generative model. The proof of Theorem 1 is available in a longer version in [28].

From Theorem 1, one can see that the MSE decreases at a rate of  $\mathcal{O}(1/\sqrt{N})$ , which is similar to those of the existing low rank matrix/tensor completion works [16, 17, 19]. In addition, the parameter  $\nu$  reflects the learning model's expressiveness. When a more complex neural network (NN) is used for modeling  $g_{\theta}$ ,  $\nu$  can be reduced—as increasing the depth/width of an NN also increases its approximation power. However, a more complex NN increases  $\tau$ . This presents a reasonable tradeoff between neural model's expressiveness, sample complexity, and recovery performance. A remark is that in our algorithm implementation, we found that not explicitly enforcing the constraints in (8) did not affect recovering the radio map, perhaps because the solutions are always bounded.

## 4. SIMULATIONS

**Problem Setup.** We consider a discretized 2D spatial region that has  $51 \times 51$  grids. The spectral domain has 64 frequency bins. The PSDs of the emitters are generated as in [1]. The SLFs are generated following the joint path loss and log-normal shadowing model from [29]. The model has two key parameters, i.e., the variance  $\omega^2$  and the decorrelation distance  $X_c$ . The shadowing effect is more severe

# Algorithm 1: Proposed Algorithm

```
\begin{array}{lll} \textbf{Data:} \ \textbf{Data:} \ \underline{Y} \in \mathbb{R}^{I \times J \times K}, \, \epsilon, \, \alpha, \, \beta, \, \text{maxIter} \\ \textbf{Result:} \ \underline{\widehat{X}} \\ \textbf{1} & \text{Initialize } \ C \text{ such that each element are uniformly distributed} \\ & \ U[0,1], \, k=1; \\ \textbf{2} & \ z_r^{(0)} \leftarrow g_{\theta}(S_r^{(0)}), \forall r \in [R]; \\ \textbf{3} & \textbf{while } \ \mathcal{L}_{\Omega,\underline{Y}}(\boldsymbol{Z}^{(k-1)},\boldsymbol{C}^{(k-1)}) \leq F_{\Omega,\underline{Y}}(\boldsymbol{Z}^{(k)},\boldsymbol{C}^{(k)}) - \epsilon \, or \\ & k > maxIter \, \textbf{do} \\ \textbf{4} & \ C^{(k+1)} \leftarrow C^{(k)} - \alpha \overline{\nabla}_C F_{\Omega,\underline{Y}}(\boldsymbol{Z}^{(k)},\boldsymbol{C}^{(k)}); \\ \textbf{5} & \ C^{(k+1)} \leftarrow \max(\boldsymbol{C}^{(k+1)},0); \text{ where } \max(\cdot,\cdot) \text{ returns} \\ & \text{elementwise maximum value.} \\ \textbf{6} & \ Z^{(k+1)} \leftarrow \boldsymbol{Z}^{(k)} - \beta \overline{\nabla}_{\boldsymbol{Z}} F_{\Omega,\underline{Y}}(\boldsymbol{Z}^{(k)},\boldsymbol{C}^{(k)}); \\ \textbf{7} & \ \textbf{for } r=1,...,R \, \textbf{do} \\ \textbf{8} & \ S_r^{(k+1)} \leftarrow g_{\theta}(\boldsymbol{z}_r^{(k+1)}); \\ \textbf{9} & \ \textbf{end} \\ \textbf{10} & \ k \leftarrow k+1; \\ \textbf{11} & \ \textbf{end} \\ \textbf{12} & \ \text{return} \ \widehat{\underline{X}} = \sum_{r=1}^R S_r^{(k)} \circ \boldsymbol{c}_r^{(k)}; \end{array}
```

if  $\omega^2$  is larger and  $X_c$  is smaller. The model also takes long-range path-loss into consideration.

Generative Model Learning. Our generative model  $g_{\theta}(\cdot)$  is learned using GAN on a variety of parameter settings for generating the SLFs; i.e., we use  $X_c$  spanning from 50 to 100,  $\omega$  taken from 2 to 7, and the long-range path-loss coefficient  $\eta$  uniformly sampled between 2 and 3 to generate the training data. We use the Adam optimizer [27] to train the network on 500,000 training samples with a batch size of 128. The algorithm runs up to 250 epochs. The initial learning rate of the discriminator and generator are set to be 0.0004 and 0.0001, respectively. We largely follow the GAN architecture from [30]. We set the latent dimension to be 256 (i.e.  $z_r \in \mathbb{R}^{256}$ ) and the output of the generator to be 51 × 51. We use sigmoid activation functions at the last layer to ensure that our generated SLF is non-negative.

**Baselines.** We use the methods from [2] and [10] (referred to as DowJons and kernel regression, respectively) as our baselines. The DowJons method in [2] also uses the deep generative model as ours but does not consider quantization [cf. Eq. (3)]. The method in [10] uses quantized measurements and multi-kernel regression. However, the method assumes that  $\boldsymbol{C}$  is known, which presents a much simpler estimation problem.

**Quantization.** In our experiments, we construct the 3-bit quantization bins  $\{b_q\}_{q=0}^8$  such that number of data lies equally in each bins. These bins are estimated from the average of 1000 radio maps [31]. We set  $\sigma^2=1.5$  throughout our experiments unless otherwise specified. For the baselines, we follow the quantization strategy in Remark 5 of [10].

**Evaluation Metric.** To evaluate the performance, we use the *log-domain normalized mean square error* (LNMSE) as our metric, which is expressed as follows: LNMSE =  $\|\widehat{\underline{M}} - \underline{M}_{\natural}\|_F^2 / \|\underline{M}_{\natural}\|_F^2$ , where  $\underline{M} = h(\underline{X})$  is the log-version of  $\underline{X}$ . Using LNMSE instead of NMSE of  $\underline{X}$  converts values to log domain that avoids over-weighting large values in  $\underline{X}$ , and thus is more reasonable when dealing with skewed data like radio maps.

**Results.** Fig. 3 shows the reconstructed radio maps on the first frequency bin. One can see that the proposed approach reconstructs a map that is visually the closest to the ground truth. The kernel regression method creates overly smooth radio maps. This could be due to a number of factors, including the fact that Gaussian kernels act as low pass filters [32]. The DowJons method that also uses deep priors does not have strong smoothing effects. However, as it does

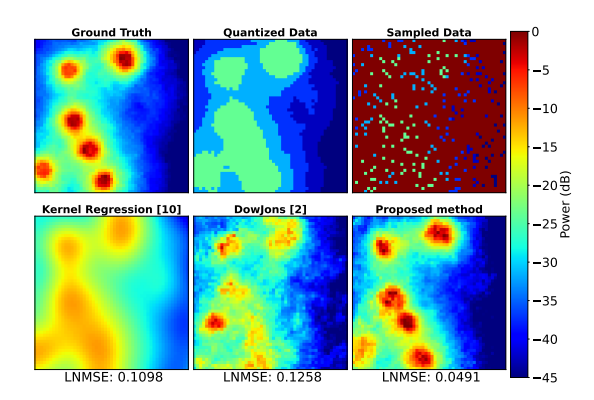


**Fig. 3**: Ground-truth and reconstructed radio maps by various methods at frequency bin 1;  $\rho = 10\%$ , R = 6,  $X_c = 50$ ,  $\omega = 4$  and  $\sigma^2 = 1.5$ , Q = 9 (3-bit quantization).

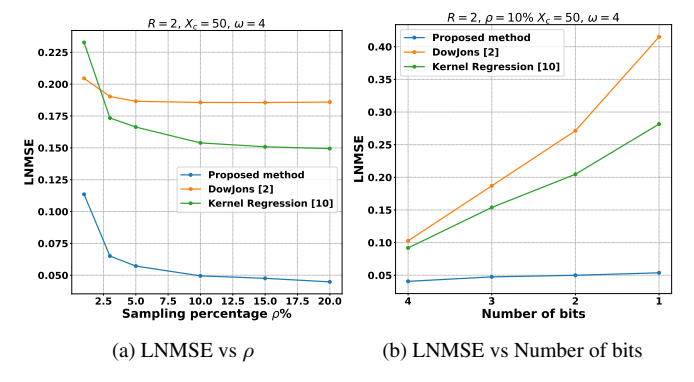


Fig. 4: LNMSEs under various conditions.

not take quantization into consideration, the recovered radio map is less accurate relative to the proposed method.

Fig 4 (a) shows the LNMSE of the reconstructed radio map under various  $\rho$ 's. The results are averaged over 20 Monte Carlo trials with different SLFs and PSDs. One can see that all methods exhibit improved performance when  $\rho$  increases, but the proposed method admits a clearly much lower LNMSE under all  $\rho$ 's relative to the baselines. This also shows that explicitly considering quantization in the formulation enhances recovery performance.

Fig 4 (b) shows the LNMSE against the number of quantization bits. Note that when the size of the quantization bins changes, the level of dithering (controlled by  $\sigma$ ) should be adjusted accordingly. To this end, we run grid search over a validation set to find  $\sigma^2$  as 2.5, 2.0, 1.5, and 0.5 for the cases using 1,2,3, and 4 bits, respectively. One can see that when the number of bits used decreases from 4 to 1, our method is barely affected, which shows robustness to heavy quantization. However, the baselines' LNMSEs deteriorates quickly when the number of bits decreases. Additional experiments can be found in the extended version of this work [28].

### 5. CONCLUSION

We considered the problem of quantized spectrum cartography and proposed a maximum likelihood formulation under a Gaussian quantization strategy. Our formulation used a deep generative model for SLFs of emitters, which is proven robust to heavy shadowing effects. We showed that our method has recoverability guarantees of the radio map tensor, even when the generative model is not perfect. Simulations supported the theoretical claims.

#### 6. REFERENCES

- G. Zhang, X. Fu, J. Wang, X.-L. Zhao, and M. Hong, "Spectrum cartography via coupled block-term tensor decomposition," *IEEE Trans. Signal Process.*, vol. 68, pp. 3660–3675, 2020.
- [2] S. Shrestha, X. Fu, and M. Hong, "Deep spectrum cartography: Completing radio map tensors using learned neural models," *IEEE Trans. Signal Process.*, vol. 70, pp. 1170–1184, 2022.
- [3] S. Bi, J. Lyu, Z. Ding, and R. Zhang, "Engineering radio maps for wireless resource management," *IEEE Wirel. Commun.*, vol. 26, no. 2, pp. 133–141, 2019.
- [4] J. A. Bazerque and G. B. Giannakis, "Distributed spectrum sensing for cognitive radio networks by exploiting sparsity," *IEEE Trans. Signal Process.*, vol. 58, no. 3, pp. 1847–1862, 2009.
- [5] G. Boccolini, G. Hernandez-Penaloza, and B. Beferull-Lozano, "Wireless sensor network for spectrum cartography based on kriging interpolation," in *Proc. IEEE PIMRC*, 2012, pp. 1565–1570.
- [6] X. Fu, N. D. Sidiropoulos, J. H. Tranter, and W.-K. Ma, "A factor analysis framework for power spectra separation and multiple emitter localization," *IEEE Trans. Signal Process.*, vol. 63, no. 24, pp. 6581–6594, 2015.
- [7] S.-J. Kim and G. B. Giannakis, "Cognitive radio spectrum prediction using dictionary learning," in *Proc. IEEE GLOBE-COM*, 2013, pp. 3206–3211.
- [8] S. Üreten, A. Yongaçoğlu, and E. Petriu, "A comparison of interference cartography generation techniques in cognitive radio networks," in *Proc. IEEE ICC*, 2012, pp. 1879–1883.
- [9] M. Hamid and B. Beferull-Lozano, "Non-parametric spectrum cartography using adaptive radial basis functions," in *Proc. IEEE ICASSP*, 2017, pp. 3599–3603.
- [10] D. Romero, S.-J. Kim, G. B. Giannakis, and R. López-Valcarce, "Learning power spectrum maps from quantized power measurements," *IEEE Trans. Signal Process.*, vol. 65, no. 10, pp. 2547–2560, 2017.
- [11] S. Niknam, H. S. Dhillon, and J. H. Reed, "Federated learning for wireless communications: Motivation, opportunities, and challenges," *IEEE Commun. Mag.*, vol. 58, no. 6, pp. 46–51, 2020.
- [12] O. Mehanna and N. D. Sidiropoulos, "Frugal sensing: Wideband power spectrum sensing from few bits," *IEEE Trans. Signal Process.*, vol. 61, no. 10, pp. 2693–2703, 2013.
- [13] A. Konar, N. D. Sidiropoulos, and O. Mehanna, "Parametric frugal sensing of power spectra for moving average models," *IEEE Trans. Signal Process.*, vol. 63, no. 5, pp. 1073–1085, 2014.
- [14] X. Fu, N. D. Sidiropoulos, and W.-K. Ma, "Power spectra separation via structured matrix factorization," *IEEE Trans. Signal Process.*, vol. 64, no. 17, pp. 4592–4605, 2016.
- [15] M. A. Davenport, Y. Plan, E. Van Den Berg, and M. Wootters, "1-bit matrix completion," *Information and Inference: A Journal of the IMA*, vol. 3, no. 3, pp. 189–223, 2014.
- [16] S. A. Bhaskar, "Probabilistic low-rank matrix completion from quantized measurements," *The Journal of Machine Learning Research*, vol. 17, no. 1, pp. 2131–2164, 2016.

- [17] Y. Cao and Y. Xie, "Categorical matrix completion," in *Proc. IEEE CAMSAP*, 2015, pp. 369–372.
- [18] C. Lee and M. Wang, "Tensor denoising and completion based on ordinal observations," in *Proc. ICML*. PMLR, 2020, pp. 5778–5788.
- [19] N. Ghadermarzy, Y. Plan, and O. Yilmaz, "Learning tensors from partial binary measurements," *IEEE Trans. Signal Pro*cess., vol. 67, no. 1, pp. 29–40, 2018.
- [20] X. Fu, S. Ibrahim, H.-T. Wai, C. Gao, and K. Huang, "Block-randomized stochastic proximal gradient for low-rank tensor factorization," *IEEE Trans. Signal Process.*, vol. 68, pp. 2170–2185, 2020.
- [21] J. A. Bazerque, G. Mateos, and G. B. Giannakis, "Group-lasso on splines for spectrum cartography," *IEEE Trans. Signal Pro*cess., vol. 59, no. 10, pp. 4648–4663, 2011.
- [22] I. Goodfellow, J. Pouget-Abadie, M. Mirza, B. Xu, D. Warde-Farley, S. Ozair, A. Courville, and Y. Bengio, "Generative adversarial nets," in *Proc. NeurIPS*, vol. 27. Curran Associates, Inc., 2014.
- [23] D. E. Rumelhart, G. E. Hinton, and R. J. Williams, "Learning internal representations by error propagation," California University San Diego, Tech. Rep., 1985.
- [24] L. Schuchman, "Dither signals and their effect on quantization noise," *IEEE Trans. Commun. Technol.*, vol. 12, no. 4, pp. 162– 165, 1964.
- [25] J. Duchi, E. Hazan, and Y. Singer, "Adaptive subgradient methods for online learning and stochastic optimization." *Journal of Machine Learning Research*, vol. 12, no. 7, 2011.
- [26] M. D. Zeiler, "ADADELTA: an adaptive learning rate method," CoRR, vol. abs/1212.5701, 2012.
- [27] D. P. Kingma and J. Ba, "Adam: A method for stochastic optimization," in *Proc. ICLR*, 2015.
- [28] S. Timilsina, S. Shrestha, and X. Fu, "Quantized radio map estimation using tensor and deep generative models," arXiv preprint arXiv:2303.01770, 2023.
- [29] A. Goldsmith, Wireless communications. Cambridge University Press, 2005.
- [30] A. Radford, L. Metz, and S. Chintala, "Unsupervised representation learning with deep convolutional generative adversarial networks," in *Proc. ICLR*, 2016.
- [31] A. S. Lan, C. Studer, and R. G. Baraniuk, "Matrix recovery from quantized and corrupted measurements," in *Proc. IEEE ICASSP*, 2014, pp. 4973–4977.
- [32] N. A. Borghese and S. Ferrari, "Hierarchical RBF networks and local parameters estimate," *Neurocomputing*, vol. 19, no. 1-3, pp. 259–283, 1998.